



## PAPER

View Article Online  
View Journal | View Issue



Cite this: *Environ. Sci.: Adv.*, 2023, 2, 1600

# The emission of low pH water from Gulf of Mexico seeps as revealed by $\delta^{13}\text{C}$ – $\text{CO}_2$ and methane oxidation data†

Sydney I. Loudon \* and John D. Kessler 

Seawater was collected around the MC118 hydrocarbon seep in the Gulf of Mexico and was used previously for a study of aerobic methane ( $\text{CH}_4$ ) oxidation. During that experiment, changes in the dissolved concentrations and  $\delta^{13}\text{C}$  isotopes of  $\text{CH}_4$  and  $\text{CO}_2$  were recorded. Originally, the  $\text{CO}_2$  concentrations and isotopes were recognized to qualitatively follow trends supporting the microbial conversion of  $\text{CH}_4$  to  $\text{CO}_2$  via aerobic oxidation, however, no attempt was made to quantitatively explain this  $\text{CO}_2$  data. The present study models the  $\delta^{13}\text{C}$ – $\text{CO}_2$  changes that occur as a result of  $\text{CH}_4$  oxidation, accounting for the carbon already present as dissolved inorganic carbon (DIC), DIC added via  $\text{CH}_4$  oxidation, and the pH of seawater. This study discovers that to accurately model the measured concentration and isotopic data for  $\text{CO}_2$ , the seawater emitted from this seep site must have a pH which is at most between 6.49 and 7.24, and possibly up to  $0.43 \pm 0.08$  pH units lower. These results are corroborated by direct measurements of pH from seeps in the Mediterranean Sea. A first-order extrapolation indicates that while cold seeps in the Gulf of Mexico may be a source of low pH water influencing the carbon dynamics of the deep ocean environment, this influence is likely less than that of current surface ocean acidification caused by the infiltration of atmospheric  $\text{CO}_2$ .

Received 3rd May 2023  
Accepted 9th October 2023

DOI: 10.1039/d3va00117b

rsc.li/esadvances

## Environmental significance

Methane seeps have been widely studied to understand the amount and fate of released methane, a potent greenhouse gas. However, this study reveals that seeps also emit low pH water, broadening the environmental significance of seafloor seeps to include ocean acidification. Using samples from a Gulf of Mexico seep, measurements and models of aerobic methane oxidation were conducted. These analyses revealed the pH of water emitted from this seep must be between 6.49 and 7.24, much lower than the average ocean pH of 8.1. This low pH water likely has important, localized influences. But a first-order extrapolation suggests the potential rate of deep ocean acidification in this environment is likely lower than the rate of seawater acidification from atmospheric  $\text{CO}_2$ .

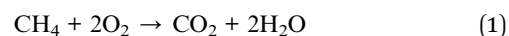
## Introduction

Seeps emit methane ( $\text{CH}_4$ ) and other hydrocarbons from the seafloor and are concentrated along continental margins. One area with many seeps that has been well documented and studied is the Gulf of Mexico, which contains an estimated 914 natural hydrocarbon seeps.<sup>1,2</sup> Both the abundance of hydrocarbons underneath the seafloor and the geology of the basin contribute to the number of seeps found in the Gulf of Mexico.<sup>3</sup>

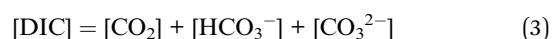
Methane is emitted from seeps in the form of dissolved  $\text{CH}_4$  and bubble streams<sup>4</sup> which can dissolve into the water column during ascent.<sup>5</sup> The rate at which these  $\text{CH}_4$  bubbles dissolve into the surrounding water depends on a variety of factors including, but not limited to, bubble size and depth of

emission<sup>6</sup> with substantial amounts of dissolution occurring near the seafloor.<sup>7</sup>

Once dissolved in the overlying waters, methanotrophic bacteria use  $\text{CH}_4$  as a carbon and energy source.<sup>8</sup> These methanotrophs are present in the water surrounding  $\text{CH}_4$  seeps and aerobically oxidize  $\text{CH}_4$  via the overall reaction shown in eqn (1).<sup>9</sup>



The  $\text{CO}_2$  produced from aerobic  $\text{CH}_4$  oxidation then mixes and equilibrates with the dissolved inorganic carbon (DIC) pool already present in the seawater (eqn (2) and (3)),



Department of Earth and Environmental Science, University of Rochester, Rochester, NY, USA. E-mail: slouden2@ur.rochester.edu

† Electronic supplementary information (ESI) available. See DOI: <https://doi.org/10.1039/d3va00117b>



where  $[CO_2]$  represents the sum of dissolved  $[CO_2]$  and  $[H_2CO_3]$ , and  $[DIC]$  is the sum of the inorganic carbon components.

The specific rate of microbial oxidation of  $CH_4$  is faster for the light isotopologue ( $^{12}CH_4$ ) than the heavy isotopologue ( $^{13}CH_4$ ), resulting in a kinetic isotope effect and producing measurable changes in the isotopic composition of the residual  $CH_4$ . Thus, the  $CO_2$  produced *via*  $CH_4$  oxidation is enriched in the  $^{12}C$  isotope compared to the residual  $CH_4$ .<sup>10</sup> These isotopic differences change as a function of the extent of oxidation and can be used to confirm that  $CH_4$  oxidation is occurring. Additionally, these changes can quantitatively determine the extent of the starting  $CH_4$  pool that has been oxidized and have been further used to determine the oxidation rate.<sup>11</sup>

The investigation presented here began with data measured during an experiment exploring aerobic  $CH_4$  oxidation in seawater.<sup>9</sup> The experiment measured changes in the dissolved concentrations and  $\delta^{13}C$  isotopes of  $CH_4$  and  $CO_2$  in a closed seawater incubation system experiencing significant amounts of aerobic  $CH_4$  oxidation.<sup>12</sup> The goal of the present study was to develop an isotopic model to quantitatively explain changes in the measured  $\delta^{13}C$ - $CO_2$  data as a function of the extent of  $CH_4$  oxidation, the results of which discovered that seeps emit relatively low pH water alongside  $CH_4$ . Variables included in this model were the isotopic fractionation associated with aerobic  $CH_4$  oxidation, the background concentrations of  $CO_2$  and DIC present in the system prior to this  $CH_4$  oxidation event, and the added  $CO_2$  from  $CH_4$  oxidation. This investigation reveals that the model and measurements only agree at pH values significantly below those of the background deep ocean, indicating that seeps are a source of low pH waters to the deep ocean.

## Experimental

### Sample collection

The full details describing sample collection and analysis can be found in Chan *et al.*<sup>9</sup> In brief, samples were collected in the Gulf of Mexico at site MC118 (28°51'N, 88°29.5'W) during a research expedition from 12–17 April 2015 onboard the E/V *Nautilus*. Samples were collected at depths of 794 and 888 m using the Suspended-Particle Rosette sampler<sup>13</sup> mounted to the remotely operated vehicle (ROV) *Hercules*. Water samples were taken just above the seafloor in water visibly impacted by  $CH_4$  bubbles. Other hydrocarbons, including oil, were present as well.<sup>9</sup>

The collected water samples were incubated at near *in situ* temperatures using a mesocosm incubation system developed by Chan *et al.*<sup>14</sup> The mesocosm incubation system was connected to a dissolved gas analysis system which measured the concentrations and stable isotopes of  $CH_4$  and  $CO_2$  throughout the incubation period. Samples for DNA analysis and cell counts were isolated periodically during incubation to characterize the microbial communities and ensure methanotrophic bacteria were present.<sup>9</sup>

### Isotope modeling procedure

Since this experiment incubated seawater samples in a closed vessel, the isotopic fractionation caused by  $CH_4$  oxidation was modeled following closed system or Rayleigh fractionation

equations.<sup>12</sup> We note that other studies of  $CH_4$  oxidation in open natural seawater environments still displayed isotopic fractionation following closed system kinetics.<sup>11,15</sup> The closed nature of the incubation vessel meant that any  $CO_2$  produced from  $CH_4$  oxidation accumulated in the vessel. Thus, to model the  $\delta^{13}C$ - $CO_2$  data, an accumulated product model was incorporated (eqn (4)).<sup>16</sup>

$$\delta_X = \frac{\delta_{CH_4,0} + 1000}{f} \left[ 1 - (1-f)^{1/\alpha} \right] - 1000 \quad (4)$$

Here,  $\delta_X$  represents the isotopic values of the accumulated  $CO_2$  produced from  $CH_4$  oxidation,  $\delta_{CH_4,0}$  represents an average of the isotopic values of  $CH_4$  at the start of the incubation, and  $\alpha$  represents the isotopic fractionation factor, defined as the ratio of the first-order rate constants for the oxidation of  $^{12}CH_4$  and  $^{13}CH_4$  ( $\alpha = k_{12}/k_{13}$ ). Previously, Chan *et al.* confirmed that  $CH_4$  oxidation followed first-order oxidation kinetics and that  $\alpha$  ranged from 1.016 to 1.025.<sup>9,12</sup> The variable  $f$  in eqn (4) represents the fraction of the starting  $CH_4$  pool that has been oxidized. Here, we determine  $f$  using the  $CH_4$  concentration data from Chan *et al.*<sup>9,12</sup> as shown in eqn (5),

$$f = 1 - \frac{[CH_4]_i}{[CH_4]_0} \quad (5)$$

where  $[CH_4]_i$  is the concentration of  $CH_4$  measured at different times throughout the incubation period, and  $[CH_4]_0$  is the averaged initial  $CH_4$  concentration. To account for variability in the data prior to the onset of more rapid  $CH_4$  oxidation, initial values of  $CH_4$  and  $CO_2$  concentrations and isotopes were averaged across several measurements.

While  $\delta_X$  represents the isotopic values of the accumulated  $CO_2$  produced during this  $CH_4$  oxidation experiment, this  $CO_2$  is added to a large pool of  $CO_2$  and DIC initially present in the seawater sample. Thus, to accurately model the measured  $\delta^{13}C$ - $CO_2$  data, a weighted isotopic average was used (eqn (6)).

$$\delta_{DIC} = \frac{[DIC]_B \delta_{DIC,B} + \Delta[CH_4] \delta_X}{[DIC]_B + \Delta[CH_4]} \quad (6)$$

Here,  $\delta_X$  represents the accumulated  $CO_2$  from eqn (4).  $\Delta[CH_4]$  represents the amount of  $CO_2$  added to the incubation from  $CH_4$  oxidation and was determined from  $[CH_4]_0 - [CH_4]_i$ . This definition assumes that all  $CH_4$  oxidized is converted to  $CO_2$ , which is likely an overestimate as some will be used to generate biomass.  $\delta_{DIC,B}$  and  $[DIC]_B$  represent the isotopic composition and concentration of DIC, respectively, in the seawater before this  $CH_4$  oxidation event. This mixing calculation is conducted with background DIC rather than background  $CO_2$  to account for any equilibration between the newly produced  $CO_2$  and the DIC system (eqn (2)). The value of  $\delta_{DIC,B}$  was determined from the initial  $\delta^{13}C$ - $CO_2$  value measured using a mass balance relationship<sup>17</sup> and experimentally determined isotopic fractionation factors.<sup>18,19</sup> At a given temperature, the isotopic fractionation between the different inorganic carbon species is a function of pH.<sup>17</sup> An initial pH was chosen to determine a possible isotopic offset between  $CO_2$  and DIC. (A full description of the calculation of the isotopic offset is provided in the ESI.†) The value of  $\delta_{DIC,B}$  was determined by adding the



calculated isotopic offset value to the initial, measured  $\delta^{13}\text{C}-\text{CO}_2$  value for each incubation experiment. On average, the values of  $\delta_{\text{CO}_2}$  were 9.38‰ lighter than the values of  $\delta_{\text{DIC}}$ .

$[\text{DIC}]_{\text{B}}$  was determined based on the dissolved  $\text{CO}_2$  concentration measurements and the pH of the seawater sample. Combining eqn (3) with the equilibrium relationships of  $K_1$  and  $K_2$  (eqn (2)) produces an equation for  $[\text{DIC}]_{\text{B}}$  as a function of  $\text{CO}_2$  concentration and pH (eqn (7)),

$$[\text{DIC}]_{\text{B}} = [\text{CO}_2]_{\text{B}} \left( 1 + \frac{K_1}{[\text{H}^+]} + \frac{K_1 K_2}{[\text{H}^+]^2} \right) \quad (7)$$

where  $K_1 = 9.558 \times 10^{-7} \text{ mol kg}^{-1}$  and  $K_2 = 5.521 \times 10^{-10} \text{ mol kg}^{-1}$  at the temperature and salinity of the incubation (7 °C and 35 ppt).<sup>20,21</sup> The value of  $[\text{CO}_2]_{\text{B}}$  is set equal to  $[\text{CO}_2]$  at the start of the incubation experiment. The pH was chosen to be equal to the value used in the isotopic offset between  $\delta_{\text{CO}_2}$  and  $\delta_{\text{DIC}}$ .

This model calculates the isotopic value of DIC in the system as a mixture of the background DIC and the DIC added from  $\text{CH}_4$  oxidation (eqn (6)). However, since values of  $\delta_{\text{CO}_2}$  were measured rather than  $\delta_{\text{DIC}}$ , the modeled values of  $\delta_{\text{DIC}}$  (eqn (6)) must be reverted to values of  $\delta_{\text{CO}_2}$  for comparison with the data. This is accomplished by subtracting the corresponding isotopic offset value calculated previously.

For each incubation experiment, the pH values incorporated into these calculations were varied until the residuals between the modeled values of  $\delta_{\text{CO}_2}$  and the measured data were minimized.

## Results and discussion

### Data and results

The modeled and measured values of  $\delta_{\text{CO}_2}$  for the four incubation experiments are shown in Fig. 1. Incubation experiments

S2 and S3 show the best agreement between the modeled and the measured values, especially during more rapid  $\text{CH}_4$  oxidation, characterized by a large drop in  $\delta^{13}\text{C}-\text{CO}_2$ . In S2 and S3, a period of positive isotopic values is followed by a rapid change to negative isotopic values. This follows the expected values where  $\delta^{13}\text{C}-\text{CO}_2$  is positive before more rapid  $\text{CH}_4$  oxidation begins and quickly becomes negative during more rapid  $\text{CH}_4$  oxidation. Incubation experiments S1 and S4 also show agreement between the data and the model, however, these samples follow a slightly different trend from S2 and S3. S1 and S4 both begin with negative isotopic values and display a steadier decline.

The pH values required to produce the isotopic models shown in Fig. 1 represent the pH at the beginning of the incubation experiment. The pH at the end of the incubation experiment was calculated using eqn (8).

$$[\text{DIC}]_{\text{F}} = [\text{CO}_2]_{\text{F}} \left( 1 + \frac{K_1}{[\text{H}^+]} + \frac{K_1 K_2}{[\text{H}^+]^2} \right) \quad (8)$$

$K_1$  and  $K_2$  are the same as in eqn (7).  $[\text{CO}_2]_{\text{F}}$  is  $[\text{CO}_2]$  at the end of the incubation experiment, and  $[\text{DIC}]_{\text{F}}$  is  $[\text{DIC}]_{\text{B}}$  plus the change in  $\text{CH}_4$ , assuming all  $\text{CH}_4$  removed was added to DIC *via*  $\text{CH}_4$  oxidation. The pH values calculated at the beginning and end of each incubation experiment are shown in Table 1.

The average difference between final and initial pH values for all four incubation experiments is  $0.1 \pm 0.07$  pH units. Overall, S1 is the most basic, and S3 is the most acidic. S2 shows no change in pH over the duration of the incubation experiment, while S4 shows the largest change. Data from all four incubation experiments suggests a pH considerably lower than the average ocean pH of 8.1.<sup>22</sup>

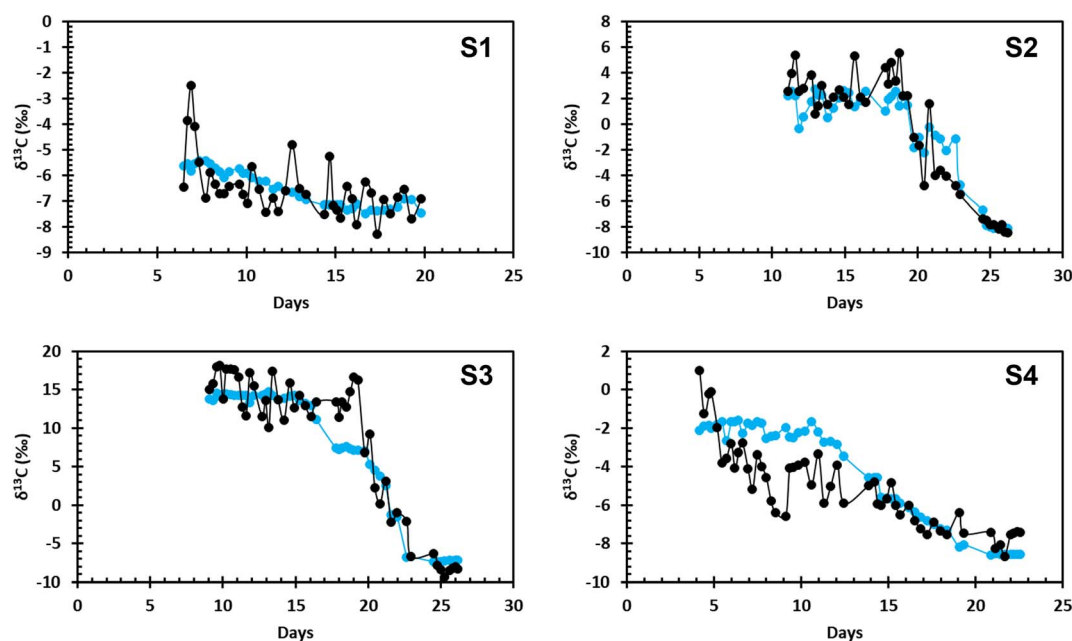


Fig. 1 The modeled  $\delta^{13}\text{C}-\text{CO}_2$  data (blue) compared to the measured values of  $\delta^{13}\text{C}-\text{CO}_2$  (black) over the incubation time for all four samples collected at MC118.



Table 1 The estimated pH range for each of the four samples

Sample	Estimated pH range
MC118-S1	7.13–7.24
MC118-S2	6.67
MC118-S3	6.49–6.62
MC118-S4	6.69–6.84

Disagreement between the modeled and measured data can be attributed to the natural variation in the measured data, differences in initial CH<sub>4</sub> concentration, oxidation of other carbon compounds in the system, and/or analytical uncertainties. The variability in the measured data is not as present in the modeled values due to the averaging of initial data before it was used in the model. Each of the four incubations had different starting concentrations of CH<sub>4</sub>. In S2 and S3, initial CH<sub>4</sub> concentrations were approximately 150 μM; in S1 and S4, initial CH<sub>4</sub> concentrations were approximately 50 μM. Methane oxidation rates were higher in S2 and S3 compared to S1 and S4. Higher initial CH<sub>4</sub> concentrations and faster oxidation rates indicate CH<sub>4</sub> oxidation was contributing more CO<sub>2</sub> to the DIC pool than in experiments S1 and S4. Oxidation of seep-derived dissolved organic carbon (DOC) would also add CO<sub>2</sub> to the DIC pool in these experiments.<sup>23</sup> Other geologic hydrocarbons were present in the incubations, which was visible at the sample collection site. Sequencing of the 16S rRNA gene at the end of each of the four incubations showed the presence of many species of hydrocarbon oxidizing bacteria, with CH<sub>4</sub> oxidizing bacteria making up a relatively low percentage of the microbial community.<sup>9</sup>

## Discussion

A pH measurement was not taken at the sampling site of this dataset, however, there is strong evidence that the water directly above the CH<sub>4</sub> seep is relatively acidic. Isotope and concentration data suggest that the pH of the sample site is between 6.49 and 7.24, if not lower. One assumption made in modeling the isotope data was that all CH<sub>4</sub> removed during the incubation experiment was converted to CO<sub>2</sub>. Based on eqn (1), two moles of O<sub>2</sub> should be removed for every mole of CH<sub>4</sub>. Dissolved O<sub>2</sub> (DO) data from Chan *et al.* indicate a DO to CH<sub>4</sub> ratio less than 2 to 1.<sup>9</sup> Chan *et al.* hypothesize that this discrepancy is due to the formation of biomass that has not been fully oxidized to CO<sub>2</sub> by the end of the incubation experiment.<sup>9</sup> Thus, if we assume that only half of the CH<sub>4</sub> is fully oxidized to CO<sub>2</sub> while the rest remains as biomass at the conclusion of this experiment, an assumption supported by the DO to CH<sub>4</sub> ratio,<sup>9</sup> the estimated pH of the water emitted from this seep is approximately 0.43 ± 0.08 pH units lower.

The pH of fluids emitted from hydrothermal vents has been well documented<sup>24,25</sup> with the development of *in situ* measurement techniques,<sup>26,27</sup> however, few measurements of pH at CH<sub>4</sub> seep sites have been published. The limited published data that exist indicate that water surrounding and coming from cold CH<sub>4</sub> seeps has an approximately neutral pH.<sup>1,28</sup> Sisma-Ventura *et al.* report measurements of pH as low as 6.83 in the water

column above a hydrocarbon seep in the Southeast Mediterranean Sea with low pH values of 6.8 to 7.4 recorded throughout the water column up to 50 m above the seafloor.<sup>28</sup>

The data and conclusions of Sisma-Ventura *et al.* support the findings of this study.<sup>28</sup> The measurement of a pH of 6.83 in the water above a hydrocarbon seep falls within the calculated pH range for the MC118 seep. The lower pH values calculated for MC118 could be attributed to the fact that water samples were collected directly above the seep emission *via* ROV whereas Sisma-Ventura *et al.* collected water up to 50 m above the seep using a carousel of Niskin bottles.<sup>28</sup>

Sisma-Ventura *et al.* conclude that the low pH values measured above hydrocarbon seeps are a result of the oxidation of CH<sub>4</sub> and other hydrocarbons to CO<sub>2</sub> which is added to the DIC pool of the background bottom water, lowering the pH.<sup>28,29</sup> Sisma-Ventura *et al.* hypothesize that hydrocarbon seeps have a substantial impact on bottom water chemistry.<sup>28</sup> The results of the present study support this conclusion and suggest that CH<sub>4</sub> seeps are a source of low pH water to the deep Gulf of Mexico.

To estimate the potential impact of this low pH water, the modeled results from this study were extrapolated to the entire Gulf of Mexico to estimate the amount of low pH water emitted and its influence on the total pH of the Gulf of Mexico. For these calculations, the Gulf of Mexico was modeled as a cylinder with a total volume of  $2.434 \times 10^{15} \text{ m}^3$  and a height equivalent to the average depth, 1615 m.<sup>30</sup> It was assumed that all estimated 914 seeps in the Gulf of Mexico<sup>2</sup> emit the same low pH water at the same, constant rate. Estimates of water flux from Gulf of Mexico seeps range from 9.4 to 30 mm per year, and seep diameters from which water is emitted are estimated to be between 0.2 and 1.2 km.<sup>31,32</sup> Maximum values were chosen for this calculation to prevent against underestimating the potential impact on bottom water pH. Therefore, the lowest pH value determined of 5.91 was used, which assumes half of the oxidized CH<sub>4</sub> remained as biomass. It was assumed that the background pH of the deep Gulf of Mexico was 8.1.<sup>22</sup> This also maximizes the estimated pH impact as the effect of low pH water emitted from seeps would be reduced in less basic surrounding water. The amount of low pH water emitted by all seeps over the span of one year was then calculated, and the resulting pH changes were determined assuming this low pH seep water impacts (i) the total volume of the Gulf of Mexico, (ii) the bottom 50 m of the Gulf of Mexico, and (iii) the bottom 10 m of the Gulf of Mexico.

Any pH change was negligible assuming the total volume or the bottom 50 m were influenced by low pH water emitted from cold seeps. When we assumed that low pH seep water only impacts the bottom 10 m of the Gulf of Mexico, the pH decreased by  $1.38 \times 10^{-4}$  in one year. For comparison, the average yearly decrease in pH from surface ocean acidification from the infiltration of atmospheric CO<sub>2</sub> is  $2.00 \times 10^{-3}$ .<sup>22</sup> Only if the water flow from all seeps in the Gulf of Mexico was higher by a factor of 10 would a similar decrease in pH be observed as in the surface waters, assuming only the bottom 10 m are impacted by seep water. A hypothetical increase in water flow by a factor of 100 would be necessary for the bottom 50 m to display a similar annual pH decrease to the surface waters. The





emission of low pH waters from CH<sub>4</sub> seeps impacts the carbon system of the deep ocean, however, the impact on deep ocean pH is likely less than the impact of acidification in the surface ocean.

## Conclusions

This study quantitatively interpreted the concentration and  $\delta^{13}\text{C}$  content of CO<sub>2</sub> measured during incubation experiments exploring aerobic CH<sub>4</sub> oxidation. The water and CH<sub>4</sub> used in this experiment were collected immediately above a Gulf of Mexico CH<sub>4</sub> seep site *via* ROV.<sup>9,12</sup> A model was developed to match the measured changes in  $\delta^{13}\text{C}$ -CO<sub>2</sub> during aerobic CH<sub>4</sub> oxidation. This model had to account for the inorganic carbon already in the system in the form of DIC as well as the CO<sub>2</sub> added from CH<sub>4</sub> oxidation.

The model reveals the importance of pH in determining the impact of added CO<sub>2</sub> on background DIC. This model and analysis suggest that the pH of water emitted at the MC118 CH<sub>4</sub> seep site is between 6.49 and 7.24 – and possibly up to 0.43 ± 0.08 pH units lower – considerably lower than the average ocean pH of 8.1.<sup>22</sup> While seeps in the Gulf of Mexico are an important source of CH<sub>4</sub>, this study proposes that they are also a source of low pH water. Based on a first-order extrapolation of the results from this isotopic model, the influence of this low pH water on the overall bottom water chemistry is relatively small, especially when compared to the rates of surface ocean acidification.

A paradox seemingly raised by these findings is the existence of authigenic carbonate formations, which are characteristic of CH<sub>4</sub> seeps,<sup>33–36</sup> surrounding an emission point of more acidic water and CH<sub>4</sub> bubbles. While we do not have a quantitative explanation for this paradox, we offer two potential avenues for future study. First, while anaerobic oxidation of methane (AOM) is the primary reaction driving authigenic carbonate precipitation,<sup>37</sup> organoclastic sulfate reduction (OSR) can also contribute to carbonate precipitation under low pH conditions<sup>38</sup> and may be contributing to carbonate precipitation in these environments. Second, beyond the point of emission of the seep itself, local sediment production and consumption of CH<sub>4</sub> may control carbonate production.<sup>39</sup> A highly localized seep environment would allow for the dual existence of both low pH water coming from the seep and authigenic carbonate formation in the surrounding environment. In addition, a previous modeling study of carbonate formation at Hydrate Ridge also suggested that carbonate can form under relatively acidic conditions with a pH of 6.9 at the sediment–water interface.<sup>40</sup>

While the regional significance of low pH water emissions from CH<sub>4</sub> seeps in the Gulf of Mexico is likely relatively minor in the context of today's environmental change, their impact on local seep environments requires further investigation. More direct measurements of the pH of water emitted from seep sites in the Gulf of Mexico and globally are needed to confirm and expand upon the findings of this study. Even if the global influence of low pH waters from CH<sub>4</sub> seeps is relatively minor compared to surface ocean acidification in the anthropocene, the results of this study highlight the need to further

characterize the influence of these low pH waters on the surrounding seafloor environment.

## Author contributions

S. L. and J. K. designed the study, performed the research, and wrote the manuscript.

## Conflicts of interest

There are no conflicts to declare.

## Acknowledgements

This research was funded by grants to J. K. from NSF (OCE-2241873 and OCE-1851402). The authors also acknowledge Eric Chan for his original collection of the data used in this study.

## Notes and references

- 1 S. B. Joye, The geology and biogeochemistry of hydrocarbon seeps, *Annu. Rev. Earth Planet. Sci.*, 2020, **48**, 205–231.
- 2 I. R. MacDonald, O. Garcia-Pineda, A. Beet, S. Daneshgar Asl, L. Feng, G. Graettinger, D. French-McCay, J. Holmes, C. Hu, F. Huffer, I. Leifer, F. Muller-Karger, A. Solow, M. Silva and G. Swayze, Natural and unnatural oil slicks in the Gulf of Mexico, *J. Geophys. Res. Oceans*, 2015, **120**, 8364–8380.
- 3 C. Fisher, H. Roberts, E. Cordes and B. Bernard, Cold seeps and associated communities of the Gulf of Mexico, *Oceanography*, 2007, **20**, 118–129.
- 4 T. C. Weber, L. Mayer, K. Jerram, J. Beaudoin, Y. Rzhano and D. Vovalv, Acoustic estimates of methane gas flux from the seabed in a 6000 km<sup>2</sup> region in the Northern Gulf of Mexico, *Geochem., Geophys., Geosyst.*, 2014, **15**, 1911–1925.
- 5 M. Leonte, B. Wang, S. A. Socolofsky, S. Mau, J. A. Breier and J. D. Kessler, Using carbon isotope fractionation to constrain the extent of methane dissolution into the water column surrounding a natural hydrocarbon gas seep in the Northern Gulf of Mexico, *Geochem., Geophys., Geosyst.*, 2018, **19**, 4459–4475.
- 6 D. F. McGinnis, J. Greinert, Y. Artemov, S. E. Beaubien and A. Wüest, Fate of rising methane bubbles in stratified waters: How much methane reaches the atmosphere?, *J. Geophys. Res. Oceans*, 2006, **111**, C09007.
- 7 B. Wang, I. Jun, S. A. Socolofsky, S. F. DiMarco and J. D. Kessler, Dynamics of gas bubbles from a submarine hydrocarbon seep within the hydrate stability zone, *Geophys. Res. Lett.*, 2020, **47**, e2020GL089256.
- 8 R. S. Hanson and T. E. Hanson, Methanotrophic bacteria, *Microbiol. Rev.*, 1996, **60**, 439–471.
- 9 E. W. Chan, A. M. Shiller, D. J. Joung, D. L. Valentine, M. C. Redmond, J. A. Breier, S. A. Socolofsky and J. D. Kessler, Investigations of aerobic methane oxidation in two marine seep environments: Part 1 – Chemical Kinetics, *J. Geophys. Res. Oceans*, 2019, **124**, 8852–8868.



- 10 J. F. Barker and P. Fritz, Carbon isotope fractionation during microbial methane oxidation, *Nature*, 1981, **293**, 289–291.
- 11 M. Leonte, J. D. Kessler, M. Y. Kellerman, E. C. Arrington, D. L. Valentine and S. P. Sylva, Rapid rates of aerobic methane oxidation at the feather edge of gas hydrate stability in the waters of Hudson Canyon, US Atlantic Margin, *Geochim. Cosmochim. Acta*, 2017, **204**, 357–387.
- 12 E. W. Chan, A. M. Shiller, D. J. Joung, E. C. Arrington, D. L. Valentine, M. C. Redmond, J. A. Breier, S. A. Socolofsky and J. D. Kessler, Investigations of aerobic methane oxidation in two marine seep environments: Part 2 – Isotopic Kinetics, *J. Geophys. Res. Oceans*, 2019, **124**, 8392–8399.
- 13 J. A. Breier, C. G. Rauch, K. McCartney, B. M. Toner, S. C. Fakra, S. N. White and C. R. German, A suspended-particle rosette multi-sampler for discrete biogeochemical sampling in low-particle-density waters, *Deep-Sea Res. I: Oceanogr. Res.*, 2009, **56**, 1579–1589.
- 14 E. W. Chan, J. D. Kessler, A. M. Shiller, D. J. Joung and F. Colombo, Aqueous mesocosm techniques enabling the real-time measurement of the chemical and isotopic kinetics of dissolved methane and carbon dioxide, *Environ. Sci. Technol.*, 2016, **50**, 3039–3046.
- 15 N. J. Grant and M. J. Whiticar, Stable carbon isotope evidence for methane oxidation in plumes above Hydrate Ridge, Cascadia Oregon Margin, *Global Biogeochem. Cycles*, 2002, **16**, 71.
- 16 J. Hoefs, *Stable Isotope Geochemistry*, Springer, Berlin, 4th edn, 1997, vol. 1, pp. 5–10.
- 17 R. E. Zeebe and D. Wolf-Gladrow, *CO<sub>2</sub> in Seawater Equilibrium, Kinetics, Isotopes*, Elsevier, Amsterdam, 2001, vol. 3, pp. 168–182.
- 18 W. G. Mook, <sup>13</sup>C in atmospheric CO<sub>2</sub>, *Neth. J. Sea Res.*, 1986, **20**, 211–223.
- 19 J. Zhang, P. D. Quay and D. O. Wilbur, Carbon isotope fractionation during gas-water exchange and dissolution of CO<sub>2</sub>, *Geochim. Cosmochim. Acta*, 1995, **59**, 107–114.
- 20 A. G. Dickson and F. J. Millero, A comparison of the equilibrium constants for the dissociation of carbonic acid in seawater media, *Deep-Sea Res., Part A*, 1987, **34**, 1733–1743.
- 21 C. Mehrbach, C. H. Culberson, J. E. Hawley and R. M. Pytkowicz, Measurement of the apparent dissociation constants of carbonic acid in seawater at atmospheric pressure, *Limnol. Oceanogr.*, 1973, **18**, 897–907.
- 22 T. Takahashi, S. C. Sutherland, D. W. Chipman, J. G. Goddard, C. Ho, T. Newberger, C. Sweeney and D. R. Munro, Climatological distributions of pH, pCO<sub>2</sub>, total CO<sub>2</sub>, alkalinity, and CaCO<sub>3</sub> saturation in the global surface ocean, and temporal changes at selected locations, *Mar. Chem.*, 2014, **164**, 95–125.
- 23 J. W. Pohlman, J. E. Bauer, W. F. Waite, C. L. Osburn and N. R. Chapman, Methane hydrate-bearing seeps as a source of aged dissolved organic carbon to the oceans, *Nat. Geosci.*, 2010, **4**, 37–41.
- 24 W. E. Seyfried Jr, N. J. Pester, B. M. Tutolo and K. Ding, The Lost City hydrothermal system: Constraints imposed by vent fluid chemistry and reaction path models on subseafloor heat and mass transfer processes, *Geochim. Cosmochim. Acta*, 2015, **163**, 59–79.
- 25 W. E. Seyfried Jr, C. Tan, X. Wang, S. Wu, G. N. Evans, L. A. Coogan, S. F. Mihály and M. D. Lilley, Time series of hydrothermal vent fluid chemistry at Main Endeavour Field, Jan de Fuca Ridge: Remote sampling using the NEPTUNE cabled observatory, *Deep-Sea Res. I: Oceanogr. Res.*, 2022, **186**, 103809.
- 26 K. Ding, W. E. Seyfried Jr, Z. Zhang, M. K. Tivey, K. L. Von Damm and A. M. Bradley, The in situ pH of hydrothermal fluids at mid-ocean ridges, *Earth Planet. Sci. Lett.*, 2005, **237**, 167–174.
- 27 C. Tan, K. Ding and W. E. Seyfried Jr, Development and Application of a New Mobile pH Calibrator for Real-Time Monitoring of pH in Diffuse Flow Hydrothermal Vent Fluids, *Mar. Technol. Soc. J.*, 2016, **50**, 37–47.
- 28 G. Sisma-Ventura, O. M. Bialik, Y. Makovsky, E. Rahav, T. Ozer, M. Kanari, S. Marmen, N. Belkin, T. Guy-Haim, G. Antler, B. Herut and M. Rubin-Blum, Cold seeps alter the near-bottom biogeochemistry in the ultraoligotrophic Southeastern Mediterranean Sea, *Deep-Sea Res. I: Oceanogr. Res.*, 2022, **183**, 103744.
- 29 P. Aharon, E. R. Graber and H. H. Roberts, Dissolved carbon and 33-133-133-1 anomalies in the water column caused by hydrocarbon seeps on the northwestern Gulf of Mexico slope, *Geo-Mar. Lett.*, 1992, **12**, 33–40.
- 30 R. E. Turner, *The Gulf of Mexico Large Marine Ecosystem*, ed. H. Kumpf, K. Steidinger and K. Sherman, Blackwell Science, Oxford, 1999, Inputs and outputs of the Gulf of Mexico, pp. 64–73.
- 31 A. J. Smith, P. B. Flemings and P. M. Fulton, Hydrocarbon flux from natural deepwater Gulf of Mexico vents, *Earth Planet. Sci. Lett.*, 2014, **395**, 241–253.
- 32 A. J. Smith, P. B. Flemings, X. Lie and K. Darnell, The evolution of methane vents that pierce the hydrate stability zone in the world's oceans, *J. Geophys. Res. Solid Earth*, 2014, **119**, 6337–6356.
- 33 A. Y. Lein, Authigenic Carbonate Formation in the Ocean, *Lithol. Miner. Resour.*, 2004, **39**, 1–30.
- 34 S. Ritger, B. Carson and E. Suess, Methane-derived authigenic carbonates formed by subduction-induced pore-water expulsion along the Oregon/Washington margin, *Geol. Soc. Am. Bull.*, 1987, **98**, 147–156.
- 35 C. K. Paull, J. P. Chanton, A. C. Neumann, J. A. Coston, C. S. Martens and W. Showers, Indicators of methane-derived carbonates and chemosynthetic organic carbon deposits: examples from the Florida Escarpment, *Palaios*, 1992, **7**, 361–375.
- 36 N. G. Prouty, D. Sahy, C. D. Ruppel, E. B. Roark, D. Condon, S. Brooke, S. W. Ross and A. W. J. Demopoulos, Insights into methane dynamics from analysis of authigenic carbonates and chemosynthetic mussels at newly-discovered Atlantic Margin seeps, *Earth Planet. Sci. Lett.*, 2016, **449**, 332–334.
- 37 W. S. Reeburgh, Oceanic Methane Biogeochemistry, *Chem. Rev.*, 2007, **107**, 486–513.



- 38 J. Blouet, S. Arndt, P. Imbert and P. Regnier, Are seep carbonates quantitative proxies of CH<sub>4</sub> leakage? Modeling the influence of sulfate reduction and anaerobic oxidation of methane on pH and carbonate precipitation, *Chem. Geol.*, 2021, **557**, 120254.
- 39 B. B. Bernard, Methane in marine sediments, *Deep-Sea Res., Part A*, 1979, **26**, 429–443.
- 40 R. Luff, K. Wallmann and G. Aloisi, Numerical modeling of carbonate crust formation at cold vent sites: significance for fluid and methane budgets and chemosynthetic biological communities, *Earth Planet. Sci. Lett.*, 2004, **221**, 337–353.

